Synoptic controls on summertime surface ozone in the northeastern United States

Jennifer Hegarty,[1] Huiting Mao,[1] and Robert Talbot[1]

Received 20 October 2006; revised 23 February 2007; accepted 27 April 2007; published 21 July 2007.

[1] The relationship between synoptic-scale circulation patterns and surface ozone (O_3) across the northeastern United States was investigated for summers 2000–2004. Observational data consisted of 1200 UT sea level pressure fields obtained from the National Centers for Environmental Prediction Global Final Analysis and O_3 measurements from 474 Environmental Protection Agency and five AIRMAP monitoring sites. The five most common circulation patterns, or map types (I–V), were identified with a correlation-based synoptic categorization technique, which persisted on 65% of the days during the study period. Map type I, characterized by stagnant warm conditions throughout the northeast, occurred most frequently (21%) with associated episodes of high O_3. Interannual variability in O_3 varied regionally from a seasonally averaged daily maximum value of 64 ppbv in 2002 to a minimum of 52 ppbv in 2004. By considering both the sea level pressure system intensity and frequency of each map type, 46% of the interannual variability in summertime O_3 was reproduced with intensity being the dominant factor. The remaining interannual variability was possibly due to nonlinear relationships between climate and biogenic emissions and/or recent reductions of power plant emissions of nitrogen oxides (NO_x) over the eastern United States. The storm track of cyclones in the eastern United States was a key determinate of the intensity of circulation patterns.

Citation: Hegarty, J., H. Mao, and R. Talbot (2007), Synoptic controls on summertime surface ozone in the northeastern United States, *J. Geophys. Res.*, *112*, D14306, doi:10.1029/2006JD008170.

1. Introduction

[2] Tropospheric ozone (O_3) is produced by complex photochemical reactions involving nitrogen oxides (NO_x which includes NO and NO_2) and hydrocarbons emitted from both anthropogenic and natural sources. The formation of O_3 is influenced strongly by climatological factors including air temperature, moisture, and solar radiation [*Seinfeld*, 1989; *Comrie and Yarnal*, 1992; *Vukovich*, 1995; *Vukovich and Sherwell*, 2003]. Atmospheric circulations exert important influence on the distribution of O_3 and its precursors on various scales, and can be especially important in modulating local meteorological controls on photochemical production and buildup of regional O_3 levels [e.g., *Li et al.*, 2002; *Vukovich and Sherwell*, 2003; *Cooper et al.*, 2002; *Mao and Talbot*, 2004; *Huntrieser et al.*, 2005].

[3] The influence of transport on the surface level O_3 has been investigated through numerous air mass trajectory studies, particularly in the northeastern United States where intensive measurement campaigns and continuous monitoring programs have helped to identify principal source regions [*Taubman et al.*, 2006; *Cooper et al.*, 2001; *Schichtel and Husar*, 2001; *Moody et al.*, 1998; *Mao and Talbot*, 2004]. However, trajectory analysis alone does not adequately reveal the climatological conditions leading to regional O_3 episodes. A comprehensive examination of circulation patterns is required to connect them with important transport trajectory pathways and ascertain critical meteorological conditions responsible for regional and local buildup of O_3.

[4] Patterns in atmospheric circulations have been categorized to determine their relationship with surface O_3 levels. For example, *Heidorn and Yap* [1986] and *Comrie and Yarnal* [1992] used manual classifications to establish that summertime high-/low-O_3 days in southern Ontario, Canada and Pittsburgh, Pennsylvania (PA) were associated with the back/front of a surface high-pressure system. *Comrie* [1992a] developed a circulation pattern sequencing technique that showed a 2–3 day succession in certain circulation types can be crucial to the formation of high-O_3 levels. *Hogrefe et al.* [2004], using the correlation-based synoptic classification technique of *Lund* [1963], identified three key sea level pressure (SLP) types over the northeast that led to high O_3 during summers 1996–2001: the Bermuda High, a high centered over the Midwest with a trough along the east coast, and a high centered directly over New England. The distribution of surface O_3 was strongly influenced by these circulation patterns, with the most widespread daily maximum O_3 associated with the Bermuda High.

[1]Institute for the Study of Earth, Oceans, and Space, Climate Change Research Center, University of New Hampshire, Durham, New Hampshire, USA.

Copyright 2007 by the American Geophysical Union.
0148-0227/07/2006JD008170

[5] Previous studies have focused mainly on the impact of different circulation patterns and their sequencing on the spatial distribution of surface O_3 for a specific episode day(s). *Comrie and Yarnal* [1992] investigated the relationship between the frequency of surface circulation types and interannual variability of surface O_3 in Pittsburgh, PA. In another study *Comrie* [1994] attributed high levels of O_3 in rural Pennsylvania during summer 1988 to unusually hot and dry conditions associated with a more northerly storm track compared to summers 1989 and 1990. However, neither study established a significant link between interannual variability in circulation patterns and surface O_3 levels.

[6] The intensity (i.e., central pressure value of a high-/low-pressure system) of a given circulation pattern and its subsequent impact on regional levels of surface O_3 is at present unexplored. The effective intensity of a circulation pattern for a given region is a function of its actual intensity, size, and relative position of its major features. For example, a Bermuda High pattern with a strong anticyclone that extends well into the central United States would have a greater effective intensity in the northeast than one with a smaller, weaker anticyclone or an anticyclone of equal strength and size but centered further east. The Bermuda High pattern with the greater effective intensity would displace the convective warm conveyor belt region of the next approaching Canadian low further west, resulting in fewer clouds, suppressed boundary layer venting and consequently poorer air quality in the northeast. In contrast, a strong Canadian high-pressure system that extends well into the United States would likely produce greater transport of cooler and presumably less polluted air (i.e., aged air) to the northeastern United States than one with a weaker high or one of equal strength positioned more northward.

[7] This study was an in-depth investigation of both the spatial and interannual relationships between surface O_3 and synoptic-scale atmospheric circulation patterns in the northeastern United States for summers 2000–2004. Our goals were to (1) identify the predominant summertime circulation patterns over the northeast, (2) establish relationships between identified circulation patterns and surface O_3 levels, (3) determine the impact of the interannual variability in circulation patterns and their intensity on surface level O_3, and (4) examine the influence of storm tracks and the number of tropical cyclones transecting the eastern United States.

2. Methods and Data

2.1. Classification of Synoptic-Scale Circulations

[8] Synoptic-scale circulation patterns over a specified region can be classified using either eigenvector-based [*Lorenz*, 1956; *Richman*, 1981; *Yarnal*, 1993] or correlation-based analyses [*Lund*, 1963; *Kirchhofer*, 1973]. The synoptic data are typically segregated on the basis of circulation commonalities and their frequency of occurrence in daily SLP or geopotential height (GPH) maps. While the eigenvector-based method is concise, the resultant component maps are not readily interpretable as real weather maps [*Yarnal*, 1993; *Yarnal et al.*, 2001].

[9] The classification of synoptic-scale circulations during our study period was conducted using the correlation-based technique [*Lund*, 1963; *Kirchhofer*, 1973]. The patterns at the surface were classified for each day during 1 June to 30 September 2000–2004. The data used here included the 1200 UT SLP fields with a resolution of 1° × 1° from the National Centers for Environmental Prediction (NCEP) Global Final Analysis (FNL) http://dss.ucar.edu/datasets/ds083.2). The map typing domain was centered over New York and Pennsylvania and covered the area from 36–48°N in latitude and 88–64°W in longitude (Figure 1).

[10] The map typing algorithm consisted of four steps. First, the correlation coefficient, r_{xy}, was calculated for each pair of grids using equation (1):

$$r_{xy} = \frac{\sum_{i=1}^{n} [(x_1 - \bar{x})(y_1 - \bar{y})]}{\left[\sum_{i=1}^{n} (x_1 - \bar{x})^2 \sum_{i=1}^{n} (y_1 - \bar{y})^2\right]^{1/2}} \quad (1)$$

where, x and y represented the SLP or GPH values at two different times at the same grid location i. The number of grid points per field was represented by n. Second, the grid that correlates with the largest number of grids at $r_{xy} > 0.7$ was identified as map type I, and this grid and all the correlated grids were removed from the matrix. Reiterations of these two steps identified five map types (I–V) before with groups at least 5% of the total number of maps could no longer be formed. The analysis was repeated one final time to provide for reassignment of a grid to a map type which may have been subsequently identified. The correlation criteria $r_{xy} > 0.7$ was determined through repeated trials which showed that for $r_{xy} < 0.7$, maps with significantly different circulation patterns could be assigned to the same category. For $r_{xy} > 0.7$ more than 10 map types were needed to classify a significant percentage (>60%) of the circulations. This finding was consistent with previous work [*Lund*, 1963; *Hogrefe et al.*, 2004; C. Hogrefe, personal communication, 2006].

2.2. Storm Track Data

[11] We further investigated links between circulation pattern intensity and interannual climate variability by examining interannual variability in storm tracks. The storm parameters were calculated from the NCAR/NCEP 2.5° × 2.5° Reanalysis (NNRA, http://www.cdc.noaa.gov/cdc/reanalysis) interpolated to an equal area 250 × 250 km grid with an algorithm based on the one described by *Serreze* [1995]. The relevant outputs consisted of the positions of all cyclones occurring over the Northern Hemisphere for the years 1958–2005. Using this data we calculated frequency and intensity statistics for each grid point to determine the major storm tracks for summers 2002 and 2004. We also examined tropical cyclone tracks available from the National Hurricane Center (NHC, http://www.nhc.noaa.gov/tracks) to determine their influence on the circulation pattern analysis. We determined the total number of tropical cyclones tracking through an expanded version of our map typing study domain and defined tropical storm days as the number of days in which a tropical system or its extratropical counterpart were located within this expanded study domain at 1200 UT. The expanded study domain consisted of the original map typing study domain of Figure 1 expanded by 5° latitude and longitude on each border.

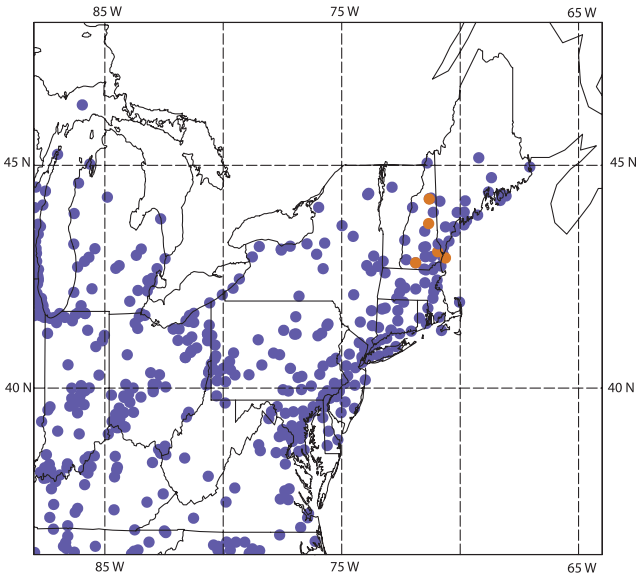

Figure 1. Map typing domain. Blue dots indicate locations of the monitoring sites from the EPA AQS observing network, and red dots indicate locations of AIRMAP stations.

2.3. Ozone, Carbon Monoxide, and $PM_{2.5}$ Data

[12] We used hourly averaged O_3 data over the time period of 1 June to 30 September 2000–2004 obtained from the Air Quality System (AQS) database (http://www.epa.gov/ttn/airs/airsaqs/) which is maintained by the Environmental Protection Agency (EPA). The O_3 data was derived from measurements at 474 monitoring sites scattered throughout the northeastern United States (Figure 1). In addition we included O_3 data from the five AIRMAP monitoring sites in New Hampshire (NH) and Maine (ME): Thompson Farm, Mount Washington Observatory, Appledore Island (ME), Pack Monadnock, and Castle Springs, which dated from April 2001 (www.airmap.unh.edu). The AIRMAP stations have site elevations ranging from sea level to 2 km, with locations designated by red circles in Figure 1.

[13] Carbon monoxide (CO) and particulate matter with an aerodynamic diameter <2.5 μm ($PM_{2.5}$) are indicative of combustion emissions. In the northeastern United States high concentrations of these species are associated with anthropogenic activities [*Mao and Talbot*, 2004], and they can serve as tracers for precursor species involved in photochemical O_3 production. Daily mean mixing ratios of CO were derived from hourly averaged observations from 172 EPA AQS sites and 1-min average data from five AIRMAP sites. Daily mean concentrations of $PM_{2.5}$ were obtained from hourly averaged observations at 133 EPA AQS sites.

3. Predominant Map Types and Associated Surface O_3 Levels

[14] Five map types corresponding to the characteristic summertime circulation patterns over the northeast are depicted in Figure 2 along with coincident distributions of O_3, CO, and $PM_{2.5}$. The O_3 maps represent the mean daily maximum values. The $PM_{2.5}$ maps represent the mean daily mean values. For CO we show the difference, ΔCO, between the daily mean for each map type and the seasonal daily mean to enhance small variations across the domain.

[15] During the study period 65% of the days had a surface circulation pattern classifiable as one of the five predominant map types (Figures 2a–2e). Map type I occurred most frequently, with 21% of the summertime days classified as this type. The map type II circulation pattern occurred on 14% of the days, map type III 11%, map type V 10%, and map type IV only 9%. The weather conditions corresponding to each map type are summarized in Table 1. Briefly, map type I was typically associated with the most widespread warm, humid, stagnant conditions throughout the northeast. Map type II generally featured mixed conditions where primarily warm and humid air extended from the southwest corner of the domain northward into western Michigan (MI). Cooler and drier air covered the region from the Upper Peninsula of MI to southern New Jersey (NJ). Map type III featured widespread cool conditions and northerly flow on the east side of the high-pressure center migrating southeast from Central Canada. Cooler conditions were also prevalent with map type IV and were accompanied by cloud cover associated with an area of low pressure in extreme western portion of the domain. Conditions associated with map type V were mixed, with warm humid air in the southwesterly flow to the east of the cold front along the east coast and cooler drier conditions in the northwesterly flow to the west of the front.

[16] The highest O_3 mixing ratios were associated with map type I (Table 2), where the domain-averaged daily maximum mixing ratio was 64 ppbv with the highest values (>70 ppbv) occurring over the east coast megalopolis extending from Washington, D.C., to Boston, Massachusetts (MA) (Figure 2f). Under map type I conditions, the northeast was largely under the influence of the Bermuda High as shown in Figure 2a. Previous studies suggest that the occurrence of pollution episodes with high O_3 levels in the eastern United States is often linked to such dynamical systems [e.g., *Seaman and Michelson*, 2000; *Gaza*, 1998].

[17] While the back edge of the Bermuda High is often an area of convection and inflow into the warm conveyor belt region of an approaching cyclone, a considerable region between the center of the high and the back edge often extends across the northeast. In this region light south-southwesterly surface flow provides a continuous supply of warm air, while cloud formation, precipitation and venting of pollutants from the boundary layer are suppressed because of synoptic-scale subsidence associated with the high. In addition, more westerly and somewhat faster flow near the top of the boundary layer can transport O_3 and precursors from the industrial and urban centers in the Midwest eastward where they can be mixed down to the surface and contribute to the buildup of high levels of O_3 along the east coast.

[18] To further illustrate the poor air quality conditions that can develop in response to suppressed boundary layer ventilation in map type I, we examined the distribution of mean daily $PM_{2.5}$ and ΔCO (Figures 2k and 2p). These species have long enough lifetimes to build up under multiday high-pressure conditions. $PM_{2.5}$ concentrations >18 μg m^{-3} and ΔCO values >20 ppbv were found in

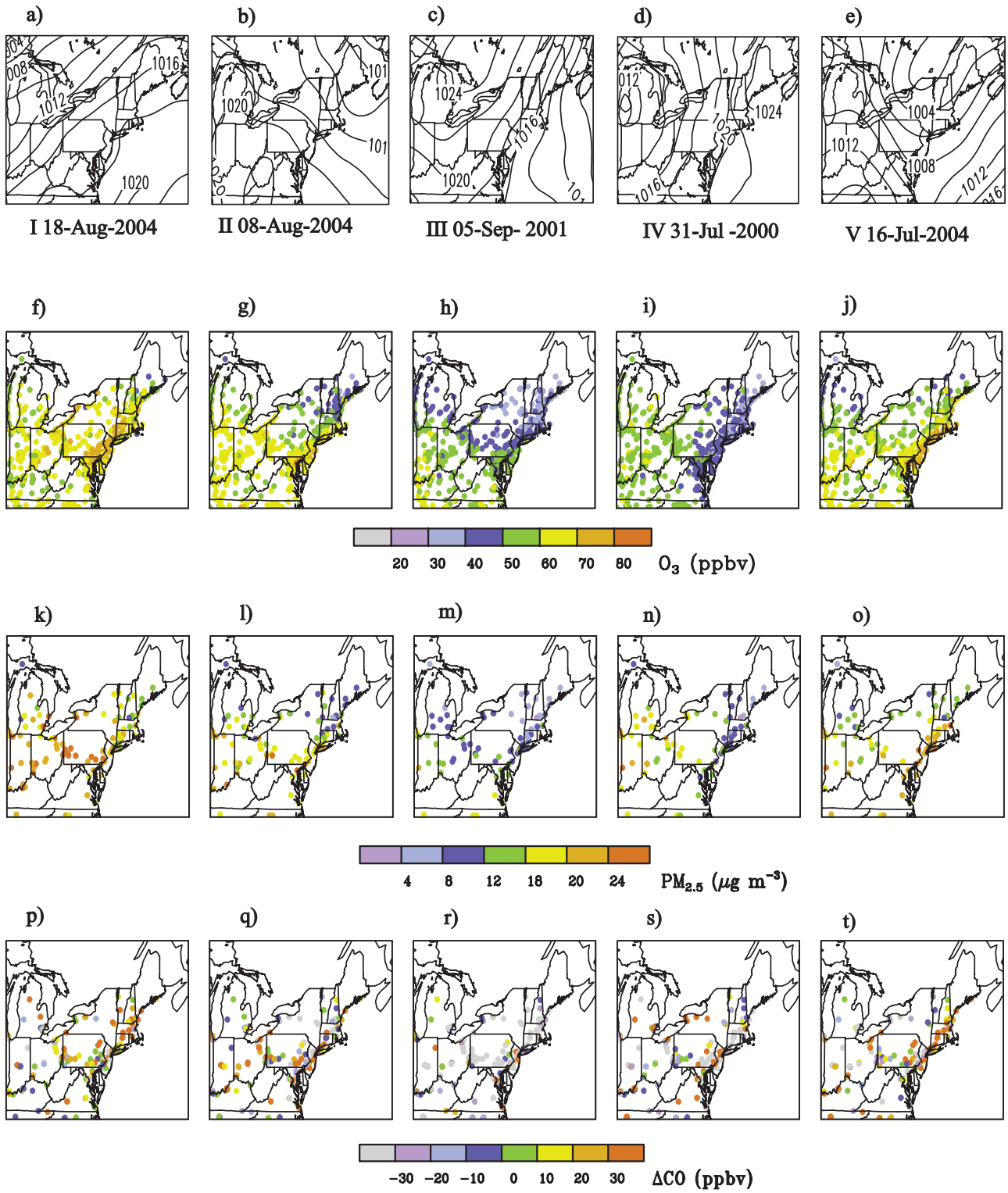

Figure 2. The representative sea level pressure (SLP) (hPa) map for map types I–V with the date listed below each plot (a–e), and, for each map type, the mean daily maximum O_3 (ppbv) (f–j), the mean daily mean $PM_{2.5}$ ($\mu g\ m^{-3}$) (k–o), and the mean daily ΔCO (ppbv) (p–t). The ΔCO is defined as the difference between the mean daily CO mixing ratio for each map type and the mean daily CO mixing ratio for all days (see section 3).

Table 1. Dominant Circulation Patterns and Meteorological Conditions for Map Types I–V

Map Type	Frequency, %	Characteristics
I	21	Bermuda High slow south and southwesterly flow at the surface (<5 m s^{-1}) veering to southwesterly and westerly flow (5–10 m s^{-1}) at the top of the boundary layer across the northeast warm and humid sporadic clouds and precipitation with isolated convection
II	14	high pressure centered over southern Ohio Valley and a trough off the coast northwesterly flow over southwestern Pennsylvania to the Virginia coastline up to northern Maine; slow southerly to southwesterly surface flow (<2 m s^{-1}) west of the Appalachians extending into the Ohio Valley northwesterly flow of 5–10 m s^{-1} at top of boundary layer over entire northeast dry and clear in northwesterly flow humid with sporadic thunderstorms in southerly flow west of the high
III	11	large high-pressure system centered north of the Upper Peninsula of Michigan northerly and northeasterly subsiding flows of 5–15 m s^{-1} throughout boundary layer clear, cool and dry
IV	9	high pressure centered east of Maine; low-pressure center or trough near western Michigan southerly and southeasterly surface flows at 3–6 m s^{-1} southwesterly flow of 5–10 m s^{-1} at top of boundary layer marine air near the coast widespread clouds and/or precipitation inland
V	10	a sharp trough extending from a low over Quebec through eastern New York and down the east coast, likely in association with a cold front southwesterly flow east of the trough; northwesterly flow west of the trough at 5–15 m s^{-1} throughout boundary layer warm and humid east of the trough; cool and dry to the west of the trough

the same regions with high O_3. This is strong evidence for a regional buildup of pollutants from air mass stagnation and unfavorable ventilation conditions.

[19] A good example of a map type I pollution scenario was the significant pollution event on 9–17 August 2002 (Figure 3). Ozone mixing ratios built up to daily 1-hour maximums exceeding 100 ppbv over a wide area extending from southern Maine (ME) to eastern Ohio (OH). Even at the relatively rural location of Thompson Farm (TF) near Durham, NH daily maximum O_3 exceeded 100 ppbv and peaked at 143 ppbv on 14 August (Figure 3a). Throughout the episode, the daily maximum temperature near the surface at TF rose from 27°C on 9 August to 36°C on 14 August, and the JNO_2 measurements suggested mostly clear sky conditions (Figures 3b–3c). The circulation for 9 August was classified as map type III, and was followed by 7 days of map type I flow. The persistent pattern finally dissipated on 17 August with the passage of a weak cold front and onset of map type V conditions (Figures 3c–3e).

[20] During the period of 10–14 August the GOES satellite images http://vortex.plymouth.edu/sat-u.html) showed a repeating diurnal cycle of mostly clear skies throughout the northeast in the morning, followed by late afternoon thunderstorms over the northwestern portion of the domain. Generally storms only propagated as far eastward as OH before dissipating in the evening hours with cloud fragments drifting into Pennsylvania (PA) and upstate New York (NY). Soundings at Albany, NY, Pittsburgh, PA, and Wilmington, OH http://vortex.plymouth.edu/get_raob-u.html) indicated a distinct synoptic-scale subsidence inversion with its base located between 2600–4000 m on the 10th, 11th, and 14th (Figure 3f). During the evening of the 13th it was much less pronounced, possibly because of dissipating cloud fragments from daytime thunderstorms in the OH area. The daily maximum hourly O_3 level west of the OH-PA border was 90–120 ppbv on 10–11 August but decreased to 50–80 ppbv by 14 August. In contrast the daily maximum hourly O_3 level east of the PA-OH border started out lower at 70–80 ppbv on 10 August and steadily rose to extreme levels on 14 August. On 14 August most of the stations along the east coast from Washington, D.C., to southern ME and westward to central PA reported daily hourly maximum O_3 mixing ratios exceeding 120 ppbv. Over the period of 15–17 August afternoon thunderstorms became more widespread in the western portion of the domain and propagated eastward as the Bermuda High retreated from the east coast. Ozone levels that were still high (50–80 ppbv inland and 80–110 ppbv along the east coast) began to decrease during this period as the effective intensity of this pattern weakened.

[21] Surface O_3 mixing ratios associated with map type II were also fairly high. Domain-averaged O_3 was 61 ppbv (Table 2), attributable to the stagnant and warm conditions to the west and south of a high-pressure system located south of the OH Valley. Under these conditions, New England, NY, northern PA, and NJ exhibited O_3 mixing ratios <60 ppbv. This resulted from northwesterly flow between the high-pressure ridge and the trough off the New England coast that brought in cooler, drier and aged Canadian air. Evidence for aged air masses under this meteorological situation is provided by $PM_{2.5}$ concentrations ≤ 12 μg m^{-3} and negative ΔCO values outside of major urban areas in New England and New York (Figure 2l).

[22] The lowest O_3 mixing ratios over the northeast occurred during time periods influenced by map types III

Table 2. Domain-Averaged O_3 Mixing Ratios for the Five Map Types[a]

Map Type	All Summers	2000	2001	2002	2003	2004
I	64.1	59.8	66.2	72.8[b]	62.6	56.2[c]
II	60.7	54.5	60.8	73.8[b]	60.8	53.4
III	50.3	47.3	49.3	55.6[c]	52.5	44.7[b]
IV	51.3	51.3	53.4[b]	51.7	50.4	50.9
V	60.1	54.6[c]	59.1	66.2[c]	63.6	54.9[c]
Unclassified	54.3	51.9	58.8	59.7	52.8	50.2
All	57.0	53.5	59.2	64.2[b]	56.5	51.7[c]

[a]Units for mixing ratios are ppbv.
[b]Departure from the 5-year mean significant at the p = 0.05 level.
[c]Departure from the 5-year mean significant at the p = 0.10 level.

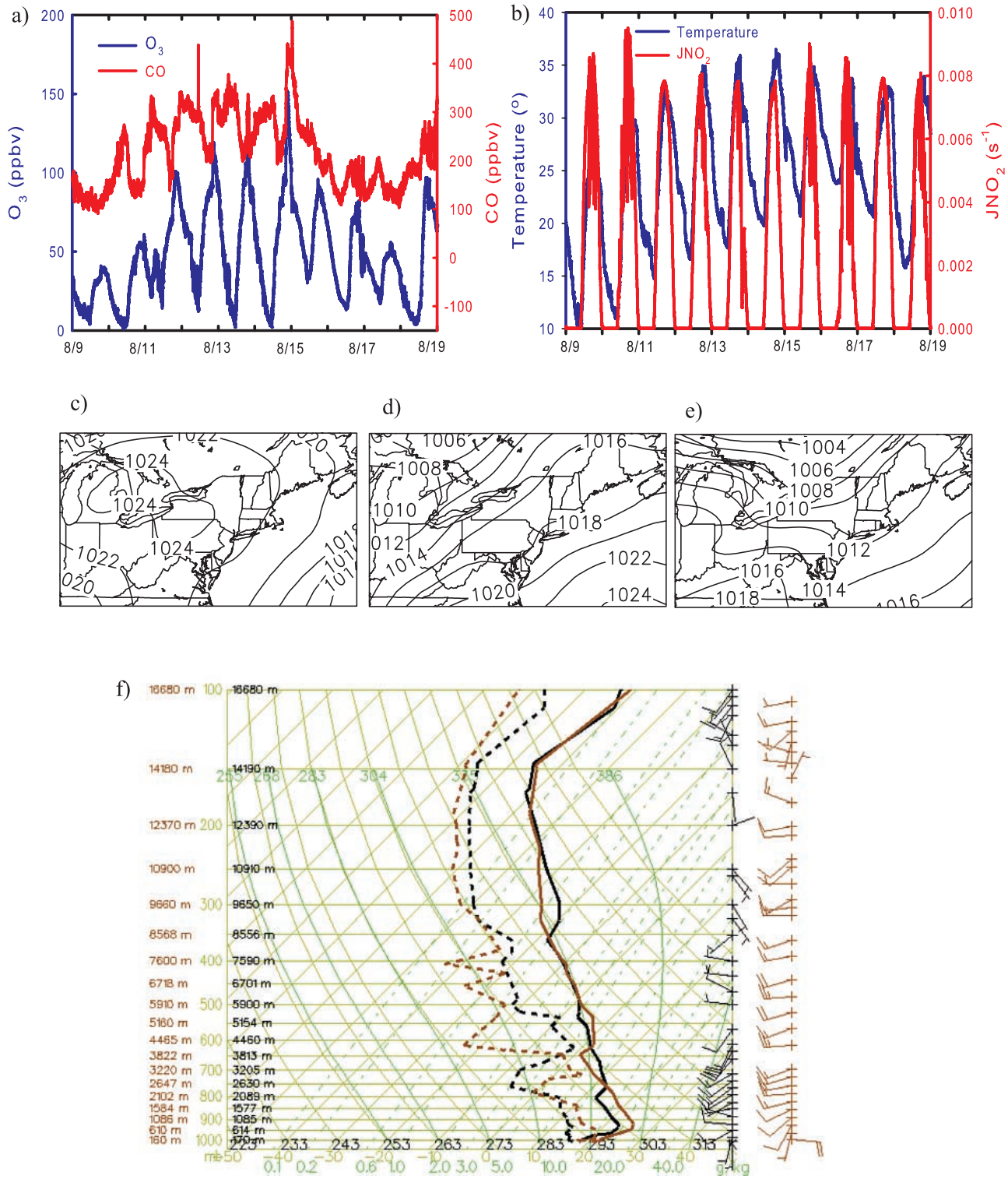

Figure 3. The August 2002 northeast pollution event; Thompson Farm time series of (a) O_3 (ppbv) and CO (ppbv) and (b) temperature (°C) and NO_2 photolysis rate (JNO_2, s^{-1}); 1200 UTC sea level pressure analysis for (c) 9 August, (d) 14 August, and (e) 18 August; (f) Skew-T Log-P sounding plot at Albany, New York, for 1200 UTC 11 August (temperature: solid black; dewpoint: dashed black) and 14 August (temperature: solid red; dewpoint: dashed red), wind barbs (knots), pressure (hPa).

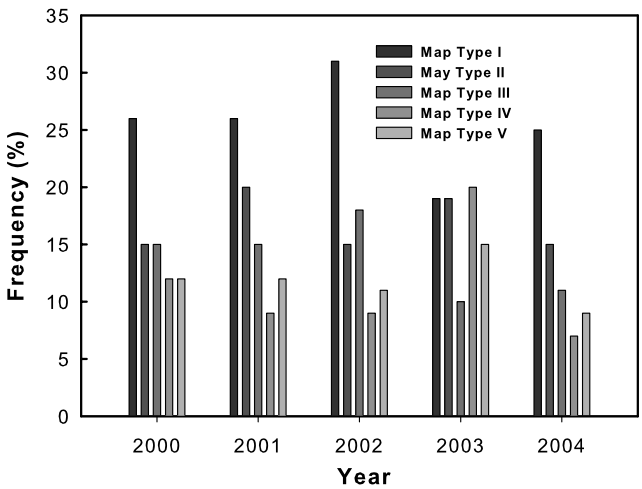

Figure 4. The frequency distribution of map types I–V for the five summers (2000–2004).

and IV, corresponding to which domain-averaged O_3 was 50 and 51 ppbv, respectively. Under map type III the high-pressure system centered over the Upper Peninsula of Michigan supplied most of the northeast with relatively aged Canadian air bearing the least anthropogenic influence as indicated by the lowest $PM_{2.5}$ and ΔCO levels (Figures 2m and 2r). For map type IV the easterly and southeasterly winds over much of the northeast transported relatively aged marine air onshore which led to decreased O_3 levels along the east coast. The persistence of reduced O_3 levels over the continent likely resulted from increased cloud cover associated with an area of low pressure in the northwestern portion of the domain.

[23] Map type V represents a transitional weather pattern from warm humid conditions to a cool drier environment in the northeast initiated by passage of a cold front trailing from a surface low in Canada. To the east of the front in New England, eastern NY, NJ, and eastern PA, southwesterly flow carrying pollutants from upwind industrial and urban centers likely increased O_3 levels in this area. West of the front, northwesterly flow from Canada funneled aged air into the region with lowered levels of O_3. The overall domain-averaged O_3 mixing ratio was 60 ppbv, ranking these pollution conditions in the middle of the five map types.

[24] The map typing analysis suggested close ties between varying synoptic-scale circulations and the spatial distribution and relative abundance of surface O_3. However, to better elucidate the contribution of circulation dynamics to the relative amounts of surface O_3, links between interannual variability of synoptic circulations and surface O_3 need to be established quantitatively.

4. Interannual Variability in Map Type Frequency and Its Impact on O_3

[25] The interannual variability in summertime surface O_3 levels during the 5-year study period is documented in Table 2. Domain-averaged O_3 reached a maximum of 64 ppbv in 2002, and decreased to a minimum of 52 ppbv in 2004. Likewise, O_3 was low at 54 ppbv in 2000, while in 2001 and 2003 it was intermediate. Student's t-tests indicated that the departure of the domain-averaged O_3 mixing ratio in 2002 from the 5-year mean was statistically significant at the $p = 0.05$ level. In 2004 it was statistically significant at the $p = 0.10$ level, while during other years the departures were not significant.

[26] Interannual variability was also observed in the frequency of surface circulation patterns (Figure 4). The summer of 2002 had the highest percentage of map type I occurrences (25%) and O_3 levels. However, 2002 also exhibited the highest percentage of map type III occurrences (15%) which were associated with low O_3 (Figure 2h). In contrast, 2004 had about the same number of map type I occurrences as did the moderate years 2000, 2001, and 2003 and actually had fewer map type III occurrences (9%) than 2002. We also examined the average persistence of each map type during the 5 years and found that there were no distinct differences between the persistence values from year to year that could explain the differences in O_3 levels. Clearly, summer O_3 concentrations are dependent on a complex interplay between ozone precursors, photochemistry, and meteorology that is not easy to predict.

[27] To quantify interannual variability captured by the surface circulation patterns, we multiplied the mean O_3 mixing ratios for each map type times the frequency of occurrence of each map type per year;

$$\overline{\overline{O_{3m}}} = \sum_{k=1}^{5} \overline{O_{3k}} F_{km} \tag{2}$$

where, $\overline{\overline{O_{3_m}}}$ is the mean O_3 mixing ratio per summer season m for the entire domain, $\overline{O_{3_k}}$ is the mean O_3 mixing ratio per map type k and F_{km} is the frequency of occurrence of map type k for summer season m. The quantity $\overline{\overline{O_{3_m}}}$ is analogous to the climatological component of the matrix operation developed by *Comrie* [1992b] to separate interannual variability of an environmental variable into its climatological (e.g., circulation types, temperature, humidity, and radiation) and environmental components (e.g., climate-induced changes in biogenic emissions and policy-mandated reductions in power plant NO_x emissions). The possible impact of the power plant NO_x reductions on O_3 levels is discussed separately in section 6.

[28] Using equation (2), the reconstructed interannual variability was nearly flat with a maximum-minimum difference of ~1 ppbv and a peak value of 59 ppbv (Figure 5). The actual interannual variability for all days showed a peak-to-peak difference of 12 ppbv with a maximum of 64 ppbv in 2002 and minimum of 52 ppbv in 2004 (Figure 5). On the basis of the frequency of map type occurrences alone, the reconstruction captured <10% of the observed variability.

[29] The reason for the poor performance of the summer O_3 reconstructions based on map type frequency may be twofold. First, there were a large number of unclassified days with high or low O_3 which were not included in our analysis. However, except for an average bias of 1.2 ppbv, the interannual variability of the mean summertime O_3 for the subset of days with classifiable circulations compared well with the interannual variability for all days (Figure 5). This result indicates that the classified days were represen-

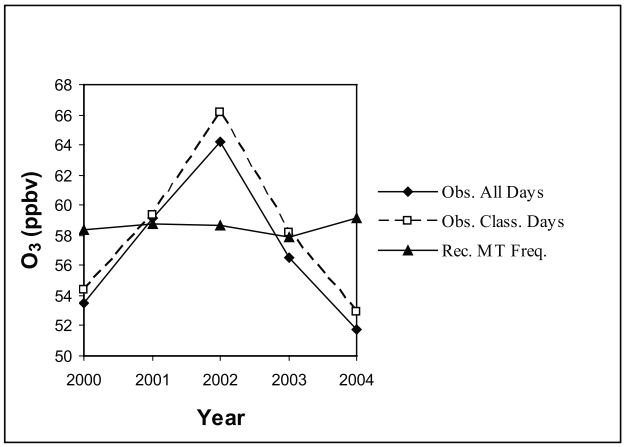

Figure 5. The domain-averaged interannual O_3 trend for the study domain for the observations on all 610 days (Obs. All Days: solid diamonds), the observations on the 396 days that had classified circulations (Obs. Class. Days: open squares), and the reconstruction from the map type frequencies according to equation (2) (Rec. MT Freq.: solid triangles).

tative of the actual interannual variability. Second, there was interannual variability of mean circulation features within each of the circulation types (hereinafter referred to as within-type) which contributed to varying O_3 levels in each map type with uncharacterized importance.

5. Linkage of Interannual Variability in Circulation Intensity With O_3

[30] On a seasonal timescale the within-type circulation variations could be depicted as differences in the mean position, size or central pressure of the dominant circulation feature (i.e., a high or low center). This was demonstrated by the mean SLP analysis for each map type as depicted in Figure 6. Small shifts in position and size are possible in the map typing classification scheme since the correlation criteria was not 1.0. In addition, differences in central pressures of circulations are not accounted for since all the grid point values are normalized by the domain mean values $\bar{x}$ and $\bar{y}$ in equation (1). Within-type circulation variations produced deviations from the mean map type meteorological and air quality conditions, thus producing an effective circulation intensity. There was apparent interannual variability in effective circulation intensity during the 5-year study period, most notably between the years 2002 and 2004.

[31] For map type I the 1020 hPa contour was much further onshore in 2002 than in any other year suggesting a more intense Bermuda High pattern which produced warmer, more stagnant and less cloudy conditions over the northeast. In contrast, the high-pressure system of map type II was weakest in 2002 with a central pressure just over 1018 hPa in the extreme southeast corner of the domain. It was strongest in 2004 with a central pressure near 1022 hPa. These characteristics resulted in weakened transport of cooler, aged Canadian air into the northeastern half of the study domain during 2002 compared to 2004.

[32] The large Canadian high pressure represented by map type III was by far the strongest in 2004, with an average central pressure near 1023 hPa and a closed 1016 hPa isobar extending to the east coast of New England and as far south as the Gulf of Mexico (expanded domain plot not shown). It also appeared strong for 2000 and 2001 but was weakened considerably in 2002 and 2003. This indicates that cooler, drier and relatively aged air was situated over much of the northeast in 2004, 2000, and 2001, in contrast to 2003 and especially 2002.

[33] For map type IV, the most striking difference was the strength of the offshore high in 2004. This system had a closed 1024 hPa isobar extending into southwestern New England and a 1020 hPa isobar protruding into the southern Appalachian Mountains. For this map type, 2004 featured cooler conditions and a greater influence of maritime air over the northeast than during any of the other years. Examination of map type V showed only minor differences in the strength of the trough along the east coast. However, the trough was somewhat deeper in 2004 as evidenced by the location of the 1014 hPa isobar which extended to just off the coast of the Carolinas, a meteorological situation that facilitates stronger and more penetrating cold fronts.

[34] We used an analysis of summertime storm tracks to further illustrate and understand interannual variability in the effective intensity of map type patterns. To do this, changes in storm track dynamics were assessed for the highly divergent years of 2002 and 2004. The track of cyclones, which facilitates Canada–United States transboundary transport as well as the North American outflow, affects the characteristics of the synoptic pressure systems over the eastern United States. Hence changes in position and frequency of these systems can impact the conditions that are relevant to regional in situ O_3 chemistry, its influx to the northeast, and subsequent export to the North Atlantic.

[35] Our examination of the storm tracks over the eastern portion of North America using NNRA cyclone frequency data revealed marked differences between the summers of 2002 and 2004 (Figure 7). In 2002 the northern Canadian storm track merged with a narrow track emanating east of the Rocky Mountains and continued eastward in a narrow band before finally merging with the east coast track east of Labrador. It was apparent that most of the continental cyclones tracked well north of our study area and cyclones along the east coast were infrequent and usually originated well offshore. On the basis of the NHC storm tracks, there were only five different tropical systems during 2002 that tracked through our domain resulting in nine tropical storm days.

[36] In contrast, during 2004 there was a weak storm track in northern Canada that merged with the Rocky Mountain track to form a broad storm track over southern Canada and the northeast. Again, many of the cyclones tracked well north of the study domain, but about a third of them tracked right along or just south of the United States–Canadian border. There was also a very active cyclone track that extended from the Gulf of Mexico, across the southeastern United States and northeastward toward Newfoundland where it merged with the southern Canadian track. Many east coast cyclones in 2004 were tropical in nature, with eight different systems transecting our domain resulting in 24 tropical storm days. The tropical storm tracks

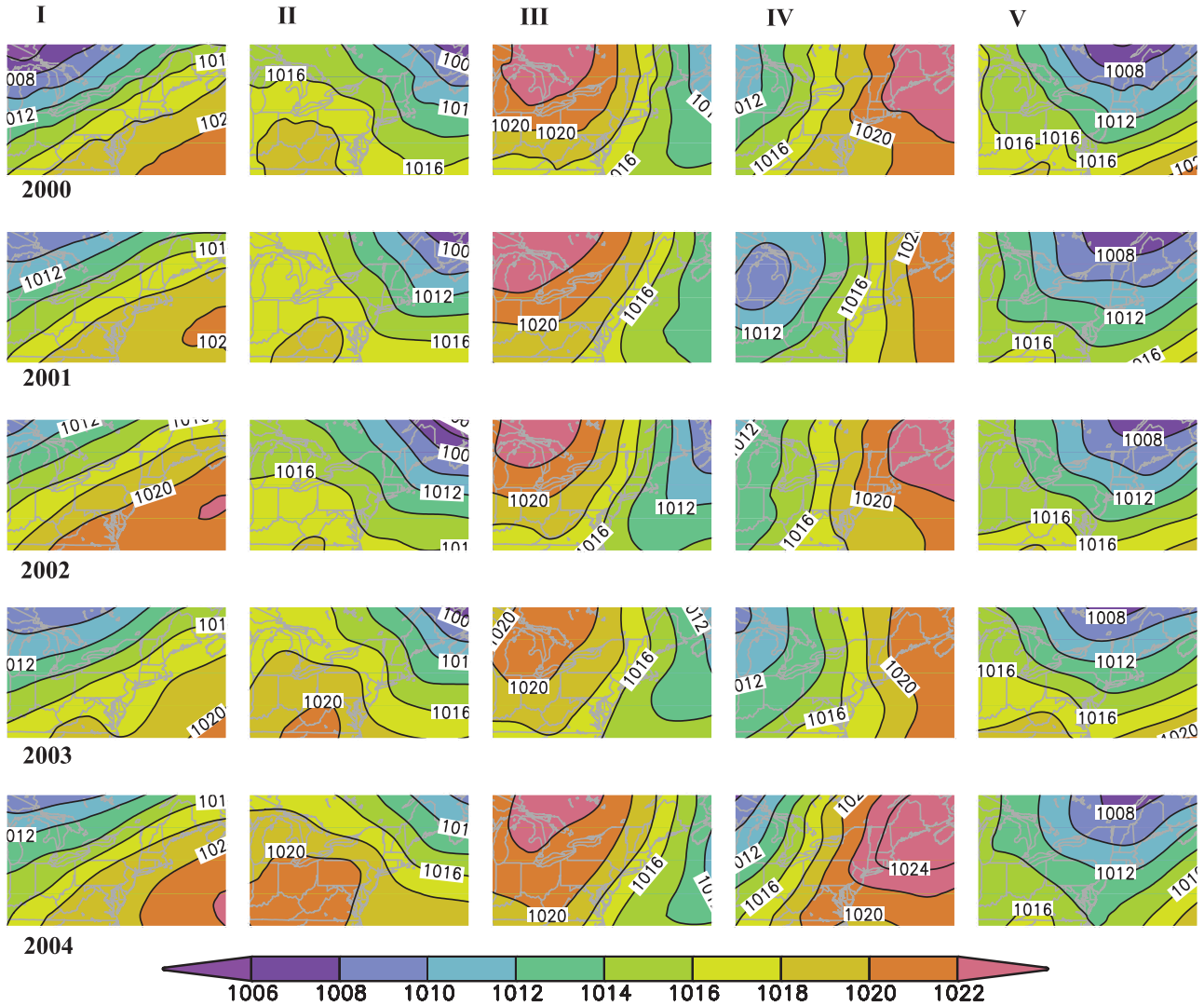

Figure 6. The Mean SLP (hPa) for each map type and summer. The year (2000–2004) of each summer appears along the left margin and the map type (I–V) is indicated at the top of each column.

for other study years were similar to those of 2002, highlighting the seemingly large and unusual influence of tropical systems on northeast circulation dynamics during 2004.

[37] The different storm tracks impacted interannual variability of the occurrence of map types and subsequently that of surface O_3 in two ways. First, the more southerly Canadian storm track and more vigorous east coast storm track in 2004 created circulation patterns that were not common to the other study years. Consequently, summer 2004 had the lowest percentage of classified days with 55%. Second, the combination of the more southerly Canadian and stronger east coast storm tracks caused cooler conditions with greater transport of aged air from Canada to the northeast. This meteorological situation acted to reduce the frequency and effective intensity of stagnant high-pressure systems over the eastern United States and minimize conditions favorable for in situ photochemical production of O_3. For example, the median mixing ratio of CO at TF was 181 ppbv in summer 2002 and 159 ppbv in 2004, along with temperatures in the northeastern United States during 2002 and 2004 that were +1.5°C warmer and −1.1°C cooler, respectively, compared to the 30-year average (1971–2000) (http://www.nrcc.cornell.edu/climate/Climate_summary.html).

6. Improved Parameterization of O_3

[38] We identified potential links to the observed interannual variability of O_3 using indices that quantified the variability of effective intensity of circulation patterns. The indices included average transport gradients, positions of key isobars, the magnitude of corresponding upper level circulation features, and domain-averaged SLP. Domain-averaged SLP was the most universal metric that could be applied readily to all map types.

[39] The physical connection of the domain-averaged pressure to the effective map type intensity should be similar for map types I–IV which are dominated by high-pressure systems. In the case of map type V, a more intense east coast trough would be reflected in a lower domain-averaged pressure. To examine this, domain-averaged pres-

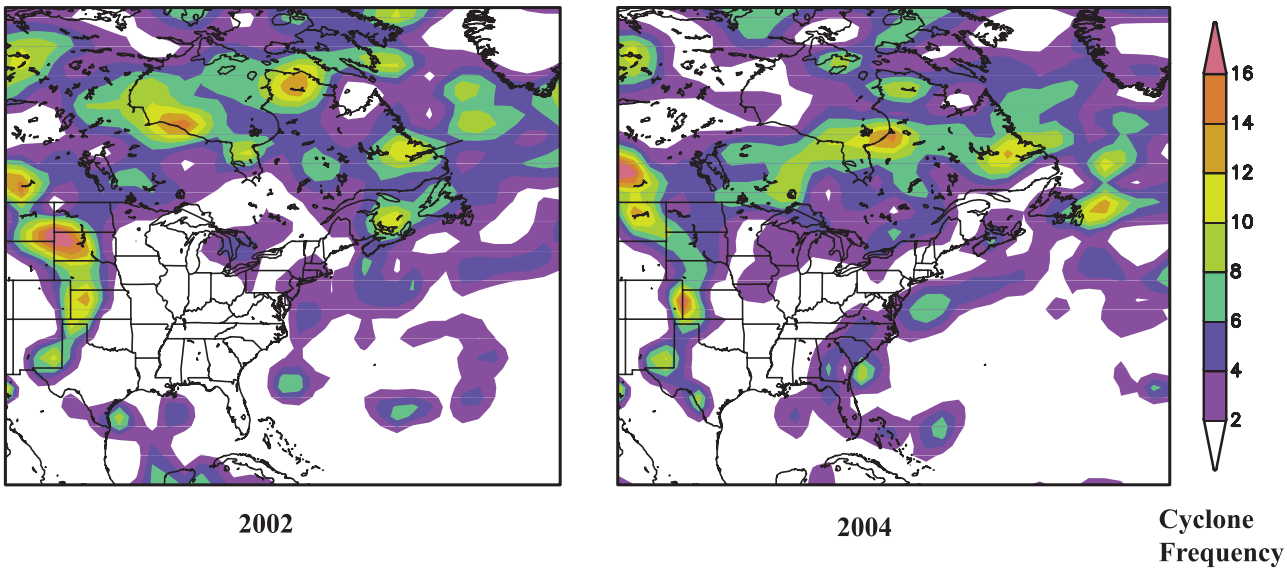

Figure 7. The frequency of cyclone centers passing through each grid point of the 250 × 250 km equal area grid for the years 2002 and 2004.

sure for each map type and year were calculated and the value termed the effective circulation intensity index (CII). Further, the quantities ΔO_3, the difference between the domain-averaged daily maximum O_3 for a given summer and the corresponding 5-year summer average were determined.

[40] We found moderate to strong linear correlations between ΔO_3 and CII for all map types except map type V (Table 3), and these results appear to be physically consistent with the circulation dynamics discussed in section 3. The weaker correlation coefficient for map type V can probably be explained by the dual role of the east coast trough which tends to increase O_3 levels on its eastern side but decrease O_3 to the west. On the basis of the linear correlations, we modified equation (2) by adding the ΔO_3 term to the reconstructed mean value for each map type;

$$\overline{\overline{O_{3m}}} = \sum_{k=1}^{5} \left(\overline{O_{3k}} + \Delta O_{3km}\right) F_{km} \tag{3}$$

The ΔO_3 value for each year was calculated from a linear fit of ΔO_3 to CII for each map type as shown in Figure 8 for map type III.

Table 3. Linear Correlation Coefficients for ΔO_3 Versus the Circulation Intensity Index for Each Map Type and for All Types Together

Map Type	Correlation Coefficient, r
I	0.55
II	−0.72
III	−0.94
IV	−0.46
V	0.23
All types	−0.17

[41] These modifications produced an interannual variability curve that was in reasonable agreement with the observed one (Figure 9). It produced a peak value of 63 ppbv in 2002 compared to the observed value of 64 ppbv for all days and 66 ppbv for classified days only. There was a decrease in 2004 to the lowest value of 57 ppbv, which was somewhat higher than the observed 52 ppbv for all days and 53 ppbv for the classified subset. Overall, the curve covered a range of 5.7 ppbv that represented ~46% of the observations for all days and 44% for classified days. Although not considered in this study, some of the observed O_3 variability was undoubtedly attributable to environmental factors such as the sensitivity of biogenic emissions to temperature and perhaps more importantly to a significant

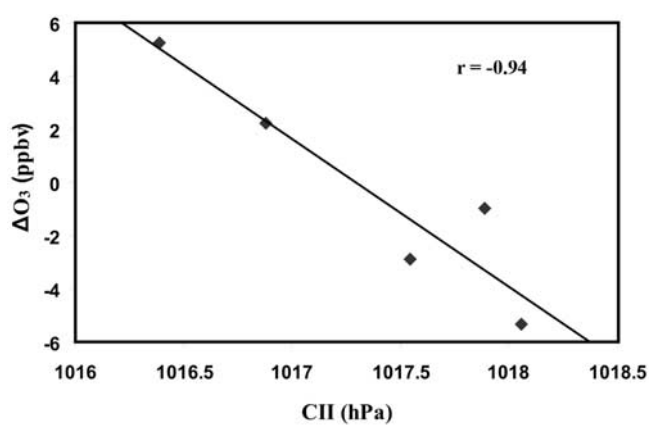

Figure 8. Scatter plot of ΔO_3 (ppbv) versus the circulation intensity index (CII, hPa) for map type III. The CII is the mean sea level pressure for the map type for a summer. The best fit line and correlation coefficient (r) appear on the plot.

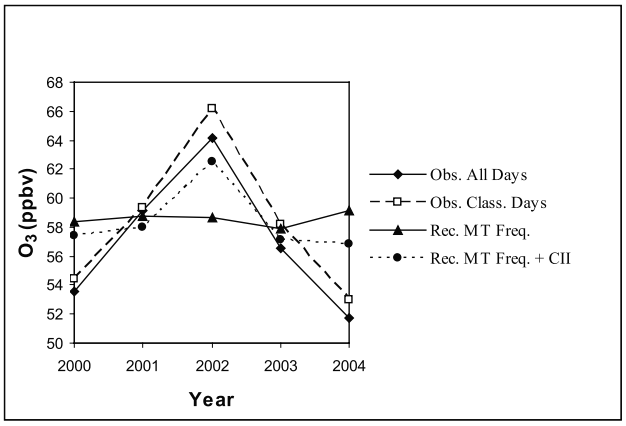

Figure 9. The domain-averaged interannual O_3 trend for the study domain for the observations on all 610 days (Obs. All Days: solid diamonds), the observations on the 396 days that had classified circulations (Obs. Class. Days: open squares), the reconstruction from the map type frequencies according to equation (2) (Rec. MT Frequation: solid triangles), and the reconstruction from map type frequencies and the CII term according to equation (3) (Rec. MT Freq. + CII: solid dots).

reduction in anthropogenic O_3 precursors during the study period.

[42] In compliance with several statutes passed in the 1990s power plants in the eastern United States reduced summertime emissions of NO_x by approximately 50% between 1999 and 2003 [*Frost et al.*, 2006]. Since 2003 the EPA estimates even greater NO_x reductions [*EPA*, 2005]. These reductions could have contributed to the dramatic drop in O_3 levels from 2002 to 2004. However, the changes in overall NO_x emissions are not clear because the NO_x emissions from mobile sources have reportedly increased at the rate of 1.9% yr^{-1} during the past 15 years [*Parrish*, 2006]. Moreover, many of the largest reductions in power plant emissions have come in typically NO_x-rich regions which would make them less effective in reducing O_3 levels. In fact, a case study by *Frost et al.* [2006] which incorporated the reduced power plant emissions into the Weather Research and Forecasting model with online Chemistry (WRF-Chem) actually showed an increase of 2 ppbv in O_3 levels over much of western Pennsylvania, Ohio, and Maryland. Thus it is difficult to directly estimate what impacts these reductions in power plant NO_x had on the O_3 interannual variability reported for our study domain.

[43] In an independent study the EPA used a statistical model to account for the impact of weather (e.g., temperature, humidity, winds) on average daily maximum 8-hour O_3 levels over the eastern United States for the May–September O_3 seasons of 2002 and 2004 [*EPA*, 2005]. The study indicated that O_3 levels were 17% lower in 2004 than in 2002, and that 41% of the total reduction in those 2 years, respectively, was due to weather; that is, it was much cooler and wetter in 2004 than in 2002. This result agrees reasonably well with our reconstructed O_3 trend based on circulation dynamics which captured 46% of the actual trend. The modest differences between the two results were likely due to a combination of factors including the choice of study domain, the use of average daily maximum 1-hour versus 8-hour O_3 level, and different statistical uncertainties in each of the techniques. Nonetheless, our results suggest that the intensity of dominant pressure systems during summertime is an important factor in understanding regional O_3 on seasonal and interannual timescales in the northeast.

7. Conclusion

[44] The five most common synoptic surface circulation patterns, referred to as map types, over the northeastern United States for summers 2000–2004 were identified objectively using a correlation-based classification technique. The highest O_3 levels over the entire northeast were associated with map type I, the most common pattern that featured the Bermuda High. Elevated O_3 levels also existed on the western side of the high-pressure system south of the Ohio Valley in Map type II. It also occurred east of an advancing cold front or the western side of a retreating anticyclone in map type V.

[45] Low O_3 levels were associated with map types III and IV which depicted an anticyclone centered over the upper Great Lakes and southern Canada, and a coastal anticyclone/Midwest cyclone or trough combination, respectively. The anticyclone of map type III appeared to suppress O_3 levels by providing air with low levels of O_3 precursors from Canada to the northeast, while the onshore winds and cloud cover associated with map type IV likely acted to further inhibit O_3 production over land.

[46] There was notable interannual variability in O_3 levels throughout the study period. The domain-averaged seasonal mean daily maximum O_3 level rose to a peak of 64 ppbv in 2002, which represented a statistically significant departure from the 5-year mean at the $p = 0.05$ level. Ozone declined to its lowest value of 52 ppbv in 2004 ($p = 0.10$ level). An improved reconstruction of O_3 interannual variability was developed by incorporating a ΔO_3 term based on the circulation intensity index for each map type. This reproduced 46% of the observed O_3 interannual variability, compared to <10% using only a frequency of occurrence term. The rest of the variability was probably due to circulations not adequately addressed by our classification procedure, environmental factors including recent reductions in power plant emissions of NO_x over the eastern United States and the impact of temperature on biogenic precursor emissions. Finally, by analyzing NCAR/NCEP Reanalysis storm tracks we demonstrated a link between interannual variability of climate and the intensity of map type patterns.

[47] There are three potential improvements which may help yield a more accurate reproduction of the interannual variability of O_3. First, increasing the number of map types by tightening the correlation criteria might strengthen the relationships between circulation and O_3 level. However, the drawback to this approach is that an increase in the number of circulation types would require much longer study periods to establish meaningful per type mean O_3 levels. This longer time period might incorporate even more changes in emission levels than occurred during the current study period which could potentially obscure the circulation-O_3 relationships. Second, interannual circulation vari-

ability may be better characterized by multiple indices rather than a single circulation intensity index. Third, the actual relationship between summertime O_3 levels and circulation might be better characterized with a nonlinear function. Future research should focus on developing more sophisticated parameterization of the relationship between the interannual variability of circulation and surface O_3.

[48] **Acknowledgments.** We would like to thank Mark Serreze of the University of Colorado for generously supplying the storm track data. Funding for this work was provided through the NOAA Office of Oceanic and Atmospheric Research as part of the AIRMAP program under grants NA03OAR4600122 and NA04OAR4600154 and also by the Environmental Protection Agency under grant RD-83145401.

References

Comrie, A. C. (1992a), An enhanced synoptic climatology of ozone using a sequencing technique, *Phys. Geogr.*, *14*, 295–316.

Comrie, A. C. (1992b), A procedure for removing the synoptic climate signal from environmental data, *Int. J. Clim.*, *12*, 177–183.

Comrie, A. C. (1994), A synoptic climatology of rural ozone pollution at three forest sites in Pennsylvania, *Atmos. Environ.*, *28*, 1601–1614.

Comrie, A. C., and B. Yarnal (1992), Relationships between synoptic-scale atmospheric circulation and ozone concentrations in metropolitan Pittsburgh, Pennsylvania, *Atmos. Environ., Part B*, *26*, 301–312.

Cooper, O. R., J. L. Moody, D. D. Parrish, M. Trainer, T. B. Ryerson, J. S. Holloway, G. Hübler, F. C. Fehsenfeld, S. J. Oltmans, and M. J. Evans (2001), Trace gas signatures of the airstreams within North Atlantic cyclones: Case studies from the North Atlantic Regional Experiment (NARE'97) aircraft intensive, *J. Geophys. Res.*, *106*, 5437–5456.

Cooper, O. R., J. L. Moody, D. D. Parrish, M. Trainer, J. S. Holloway, G. Hübler, F. C. Fehsenfeld, and A. Stohl (2002), Trace gas composition of midlatitude cyclones over the western North Atlantic Ocean: A seasonal comparison of O_3 and CO, *J. Geophys. Res.*, *107*(D7), 4057, doi:10.1029/2001JD000902.

Environmental Protection Agency (2005), Evaluating ozone control programs in the eastern United States: Focus on the NO_x budget trading program, *Rep. EPA454-K-05-001,* 35 pp., Washington, D. C. (Available at http://www.epa.gov/airtrends/2005/ozonenbp.pdf)

Frost, G. J., et al. (2006), Effects of changing power plant NOx emissions on ozone in the eastern United States: Proof of concept, *J. Geophys. Res.*, *111*, D12306, doi:10.1029/2005JD006354.

Gaza, R. S. (1998), Mesoscale meteorology and high ozone in the northeastern United States, *J. Appl. Meteorol.*, *37*, 961–977.

Heidorn, K. C., and D. Yap (1986), A synoptic climatology for surface ozone concentrations in southern Ontario, 1976–1981, *Atmos. Environ.*, *20*, 695–703.

Hogrefe, C., et al. (2004), Simulating regional-scale ozone climatology over the eastern United States: Model evaluation results, *Atmos. Environ.*, *38*, 2627–2638.

Huntrieser, H., et al. (2005), Intercontinental air pollution transport from North America to Europe: Experimental evidence from airborne measurements and surface observations, *J. Geophys. Res.*, *110*, D01305, doi:10.1029/2004JD005045.

Kirchhofer, W. (1973), Classification of European 500 mb patterns, *Arbeitsber. Schweiz. Meteorol. Zentralanst.*, *43*, 205–207.

Li, Q., et al. (2002), Transatlantic transport of pollution and its effects on surface ozone in Europe and North America, *J. Geophys. Res.*, *107*(D13), 4166, doi:10.1029/2001JD001422.

Lorenz, E. N. (1956), Empirical orthogonal functions and statistical weather prediction, *Sci. Rep. 1,* Meteorol. Dep., Mass. Inst. of Technol., Cambridge.

Lund, I. A. (1963), Map-pattern classification by statistical methods, *J. Appl. Meteorol.*, *2*, 56–65.

Mao, H., and R. Talbot (2004), Role of meteorological processes in two New England ozone episodes during summer 2001, *J. Geophys. Res.*, *109*, D20305, doi:10.1029/2004JD004850.

Moody, J. L., J. W. Munger, A. H. Goldstein, D. J. Jacob, and S. C. Wofsy (1998), Harvard Forest regional-scale air mass composition by Patterns in Atmospheric Transport History (PATH), *J. Geophys. Res.*, *103*, 13,181–13,194.

Parrish, D. D. (2006), Critical evaluation of US on-road vehicle emission inventories, *Atmos. Environ.*, *40*, 2288–2300, doi:10.1016/j.atmosenv.2005.11.033.

Richman, M. B. (1981), Obliquely rotated principal components: An improved meteorological map typing technique?, *J. Appl. Meteorol.*, *20*, 1145–1159.

Schichtel, B. A., and R. B. Husar (2001), Eastern North American transport climatology during high- and low-ozone days, *Atmos. Environ.*, *35*, 1029–1038.

Seaman, N., and S. Michelson (2000), Mesoscale meteorological structure of a high-ozone episode during the 1995 NARSTO-Northeast study, *J. Appl. Meteorol.*, *39*, 384–398.

Seinfeld, J. H. (1989), Urban air pollution: State of the science, *Science*, *243*, 745–752.

Serreze, M. C. (1995), Climatological aspects of cyclone development and decay in the Arctic, *Atmos. Ocean*, *33*, 1–23.

Taubman, B. F., J. C. Hains, A. M. Thompson, L. T. Marufu, B. G. Doddridge, J. W. Stehr, C. A. Piety, and R. R. Dickerson (2006), Aircraft vertical profiles of trace gas and aerosol pollution over the mid-Atlantic United States: Statistics and meteorological cluster analysis, *J. Geophys. Res.*, *111*, D10S07, doi:10.1029/2005JD006196.

Vukovich, F. M. (1995), Regional-scale boundary layer ozone variations in the eastern United States and their association with meteorological variations, *Atmos. Environ.*, *29*, 2259–2273.

Vukovich, F. M., and J. Sherwell (2003), An examination of the relationship between certain meteorological parameters and surface ozone variations in the Baltimore-Washington corridor, *Atmos. Environ.*, *37*, 971–981.

Yarnal, B. (1993), *Synoptic Climatology in Environmental Analysis: A Primer*, 195 pp., Bellhaven, London.

Yarnal, B., A. C. Comrie, B. Frakes, and D. P. Brown (2001), Developments and prospects in synoptic climatology, *Int. J. Climatol.*, *21*, 1923–1950.

J. Hegarty, H. Mao, and R. Talbot, Institute for the Study of Earth, Oceans, and Space (EOS), Climate Change Research Center, University of New Hampshire, Morse Hall, 39 College Road, Durham, NH 03824-3525, USA.